

Title	Direct imaging of structural heterogeneity of the melt-spun $\text{Fe}_{85.2}\text{Si}_2\text{B}_8\text{P}_4\text{Cu}_{0.8}$ alloy
Author(s)	Sato, Kazuhisa; Takenaka, Kana; Makino, Akihiro et al.
Citation	AIP Advances. 5(6) p.067166
Issue Date	2015-06
oaire:version	VoR
URL	https://hdl.handle.net/11094/89407
rights	This article is licensed under a Creative Commons Attribution 3.0 Unported License.
Note	

Osaka University Knowledge Archive : OUKA

<https://ir.library.osaka-u.ac.jp/>

Osaka University



Direct imaging of structural heterogeneity of the melt-spun Fe_{85.2}Si₂B₈P₄Cu_{0.8} alloy

Kazuhisa Sato, Kana Takenaka, Akihiro Makino, and Yoshihiko Hirotsu

Citation: *AIP Advances* **5**, 067166 (2015); doi: 10.1063/1.4923329

View online: <http://dx.doi.org/10.1063/1.4923329>

View Table of Contents: <http://scitation.aip.org/content/aip/journal/adva/5/6?ver=pdfcov>

Published by the *AIP Publishing*

Articles you may be interested in

Evolution of fcc Cu clusters and their structure changes in the soft magnetic Fe_{85.2}Si₁B₉P₄Cu_{0.8} (NANOMET) and FINEMET alloys observed by X-ray absorption fine structure

J. Appl. Phys. **117**, 17A324 (2015); 10.1063/1.4916937

Phase transition from fcc to bcc structure of the Cu-clusters during nanocrystallization of Fe_{85.2}Si₁B₉P₄Cu_{0.8} soft magnetic alloy

AIP Advances **4**, 057129 (2014); 10.1063/1.4880241

Magnetic properties and structure of Fe_{83.3}–85.8B_{7.0}–4.5P₉Cu_{0.7} nanocrystalline alloys

J. Appl. Phys. **113**, 17A311 (2013); 10.1063/1.4794377

Role of Si in high Bs and low core-loss Fe_{85.2}B₁₀–XP₄Cu_{0.8}Si_x nano-crystalline alloys

J. Appl. Phys. **112**, 103902 (2012); 10.1063/1.4765718

High coercivity of melt-spun (Fe 0.55 Pt 0.45) 78 Zr 2–4 B 18–20 nanocrystalline alloys with L1 0 structure

J. Appl. Phys. **95**, 7498 (2004); 10.1063/1.1676037

An advertisement for AIP's Journal of Computational Tools and Methods. The background shows a row of computer monitors in a library or office setting, each displaying a colorful, abstract image. The text 'AIP'S JOURNAL OF COMPUTATIONAL TOOLS AND METHODS. AVAILABLE AT MOST LIBRARIES.' is overlaid in white and yellow. The 'Computing' logo is also present in the bottom right corner.

Computing
SCIENCE ENGINEERING

AIP'S JOURNAL OF COMPUTATIONAL TOOLS AND METHODS.
AVAILABLE AT MOST LIBRARIES.

Direct imaging of structural heterogeneity of the melt-spun $\text{Fe}_{85.2}\text{Si}_2\text{B}_8\text{P}_4\text{Cu}_{0.8}$ alloy

Kazuhiro Sato,^{1,a} Kana Takenaka,¹ Akihiro Makino,¹ and Yoshihiko Hirotsu²

¹Institute for Materials Research, Tohoku University, Sendai 980-8577, Japan

²Institute of Scientific and Industrial Research, Osaka University, Ibaraki 567-0047, Japan

(Received 1 May 2015; accepted 18 June 2015; published online 26 June 2015)

A structural heterogeneity of the melt-spun $\text{Fe}_{85.2}\text{Si}_2\text{B}_8\text{P}_4\text{Cu}_{0.8}$ alloy has been studied by spherical aberration (C_s) corrected high-resolution transmission electron microscopy. Hollow-cone illumination imaging revealed that the density of coherent scattering regions in the as-quenched $\text{Fe}_{85.2}\text{Si}_2\text{B}_8\text{P}_4\text{Cu}_{0.8}$ alloy is much higher than that in the $\text{Fe}_{76}\text{Si}_9\text{B}_{10}\text{P}_5$ bulk metallic glass. According to the C_s -corrected TEM, crystalline atomic clusters, typically of ~ 1 nm in diameter, are densely distributed in an amorphous matrix of $\text{Fe}_{85.2}\text{Si}_2\text{B}_8\text{P}_4\text{Cu}_{0.8}$ alloy. Observation of four-fold and six-fold atomic arrangements of these clusters implies existence of Fe clusters with the body centered cubic structure. These Fe clusters must be responsible for the formation of ultrahigh-density α -Fe nanocrystals produced by post-annealing. © 2015 Author(s). All article content, except where otherwise noted, is licensed under a Creative Commons Attribution 3.0 Unported License. [<http://dx.doi.org/10.1063/1.4923329>]

Iron (Fe) based nanocrystalline soft magnetic materials have been developing for long years by tuning alloy composition and constituent elements.¹⁻³ The newly developed FeSiBPCu nanocrystalline soft magnetic alloy contains more than 83at%Fe, and exhibits excellent soft magnetic properties with a high saturation magnetization after a proper heat treatment of an as-quenched ribbon ($H_c = 7-10$ A/m, $B_s = 1.88-1.94$ T).^{4,5} The Fe content exceeds the upper limit (~ 80 at%) required for single amorphous phase formation for soft magnetic Fe-Si-B-P metallic glass; hence it is probable that the as-quenched alloy must contain crystalline clusters, forming “hetero-amorphous” structure.^{4,5} The preceding studies have shown^{4,5} a sign of the presence of crystalline clusters, while detailed atomic structure characterization has not been performed yet. It has been suggested that possible “pre-existing” Fe clusters formed at the as-quenched state could act as nucleation site for the α -Fe grains with the body centered cubic (bcc) structure during the crystallization of hetero-amorphous structure.⁴ Also note that the pre-existing nuclei and the newly formed nuclei in the annealing process will grow together, which has been proposed based on thermal analysis as a function of heating rate.⁶ Such a simultaneous growth of two kinds of nuclei will prevent grain growth and lead to the formation of high-density α -Fe grains with smaller grain sizes. The excellent soft magnetic properties of the FeSiBPCu nanocrystalline alloy can be attributed to the high-density α -Fe nanocrystals as well as the high Fe content. However, atomic scale structural details of the as-quenched FeSiBPCu alloy still remain an open question.

To characterize atomic structures unambiguously, spherical aberration (C_s) corrected high-resolution transmission electron microscopy (HRTEM) is a suitable technique in respect of spatial resolution (~ 0.1 nm). In addition to highly improved spatial resolution, C_s -corrected TEM has a benefit of smaller defocus values under optimal defocus conditions, which is beneficial for imaging extremely small atomic clusters. The purpose of this study is to reveal atomic structures of a melt-spun $\text{Fe}_{85.2}\text{Si}_2\text{B}_8\text{P}_4\text{Cu}_{0.8}$ alloy, especially in relation to the proposed hetero-amorphous structure.

FeSiBPCu alloy ingots were prepared by induction melting of Fe (99.98 mass%), Si (99.998 mass%), B (99.5 mass%), Cu (99.99 mass%) and premelted Fe-P (99.9 mass%) in a high purity

^aElectronic mail: ksato@imr.tohoku.ac.jp



Argon (Ar) atmosphere. Then, rapidly solidified FeSiBPCu ribbons with 10 mm in width and $\sim 13 \mu\text{m}$ in thickness were prepared using the aforementioned ingots by a single-roller melt-spinning method in air. Plan-view TEM specimens were prepared by a mechanical polishing in ethanol using a $0.3 \mu\text{m}\text{-Al}_2\text{O}_3$ wrapping film followed by a low voltage Ar-ion milling at low temperatures ($\sim 180 \text{ K}$). For atomic structure imaging using a 300 kV-TEM (FEI Titan80-300), the C_s was adjusted to approximately $-1 \mu\text{m}$. Theoretical optimal defocus required for atomic structure imaging is as small as 1.6 nm in the present experimental condition, which can effectively minimize imaging artifact. Possible structural change due to electron irradiation can be excluded in the HRTEM observation using a CCD camera with a short acquisition time of 1 s or less.⁷ Nanobeam electron diffraction (NBED) patterns were obtained by scanning $\sim 0.1 \text{ nm}$ -sized electron probe using a 200 kV-TEM with a cold field emission gun (JEOL JEM-ARM200F).

Figure 1(a) shows a hollow-cone dark-field (DF) TEM image of an as-quenched $\text{Fe}_{85.2}\text{Si}_2\text{B}_8\text{P}_4\text{Cu}_{0.8}$ alloy. An attached selected area electron diffraction (SAED) pattern obtained from a wide area ($\sim 700 \text{ nm}$ in diameter) shows only halo rings arising from amorphous structure. Intensity from the first halo ring selected by a small objective aperture ($10 \mu\text{m}$ in diameter) was employed for the hollow-cone DF-TEM imaging. In this study, electron beam was deflected in the radial direction and then rotated in the circumference direction. Thus, all the intensity from the first halo ring was incorporated in a DF-TEM image. In Fig. 1(a), bright contrast so called “speckle” comes from a distribution of medium-range order (MRO) in an amorphous structure.^{8,9} For comparison, a

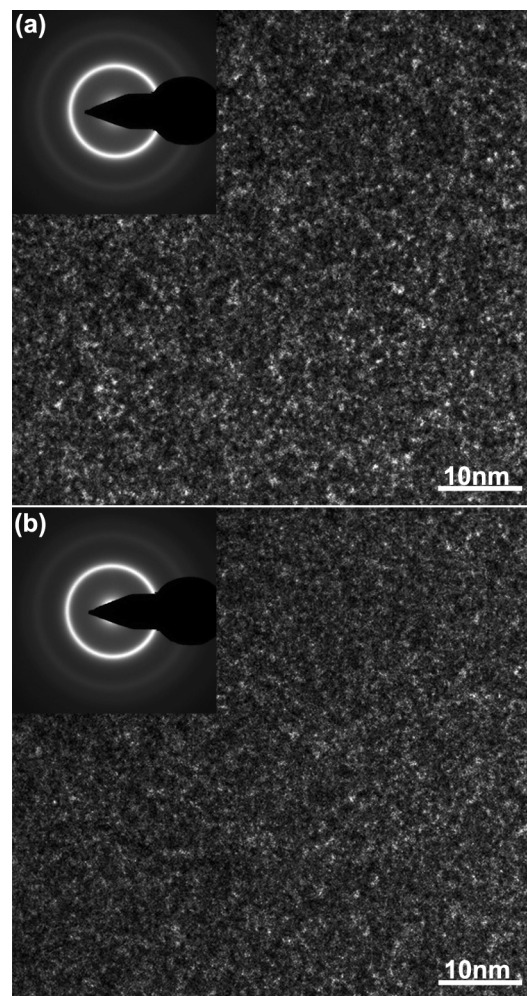


FIG. 1. Hollow-cone DF-TEM images and the corresponding SAED patterns of as-quenched (a) $\text{Fe}_{85.2}\text{Si}_2\text{B}_8\text{P}_4\text{Cu}_{0.8}$ hetero-amorphous alloy and (b) $\text{Fe}_{76}\text{Si}_9\text{B}_{10}\text{P}_5$ bulk metallic glass.

hollow-cone DF-TEM image and the corresponding SAED pattern of an as-quenched $\text{Fe}_{76}\text{Si}_9\text{B}_{10}\text{P}_5$ bulk metallic glass with single amorphous phase are also shown in Fig. 1(b). As seen, the areal number density of strong speckled-contrasts is apparently higher in the FeSiBPCu alloy than in the bulk metallic glass. Thus, DF-TEM imaging clearly reveals the presence of a highly heterogeneous structure presumably of atomic clusters (MRO regions) in the FeSiBPCu alloy, while their detailed structure is unknown. To clarify the atomic structure of such high-density speckles, we have performed C_s -corrected TEM observation.

Figure 2 shows a C_s -corrected HRTEM image of an as-quenched $\text{Fe}_{85.2}\text{Si}_2\text{B}_8\text{P}_4\text{Cu}_{0.8}$ alloy. An attached SAED pattern shows only halo-rings arising from amorphous structure. However, small atomic ordered regions are observed in the encircled area. As can be seen, there is a size distribution of such local ordered regions ranging from 1 nm to about 2.5 nm. By using the image simulation technique applied for amorphous structures,^{10,11} it has been well demonstrated that an ordered region of bright spots (or dark spots, depending on the defocus condition) appearing in the HRTEM image of amorphous alloy under a suitable imaging condition comes from a local atomic ordered region in the alloy. Because of the locally confined crystalline structure, we occasionally call these local ordered regions “crystalline (atomic) clusters”.

In Fig. 2(a), deformed images of ordered regions are often seen as shown in the white bold-circles. Also, we often observe eucentric onion-like contrasts (see in the white thin circle with a single arrow). Because of the embedded crystalline clusters are thought to be strongly deformed, and also a fairly strong orientation dependence is expected for the clear imaging of crystalline clusters, statistically, it is not easy to obtain clear high contrast local crystalline cluster images

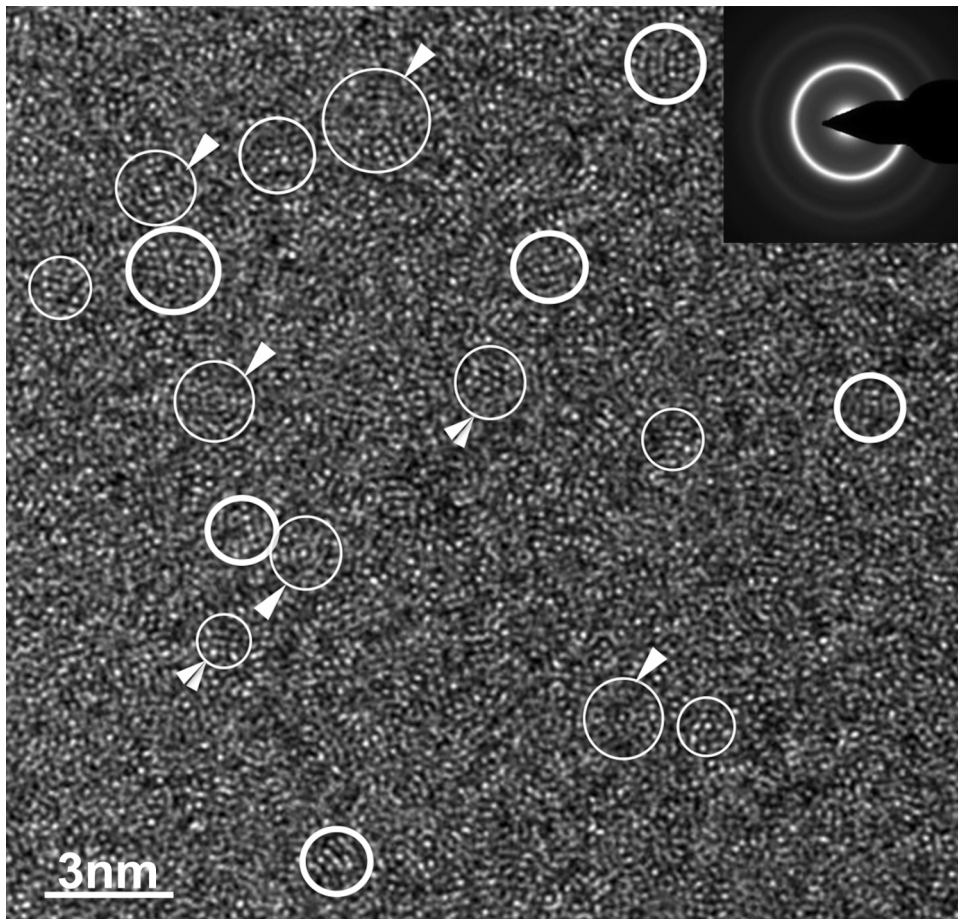


FIG. 2. C_s -corrected HRTEM image and a corresponding SAED pattern of an as-quenched $\text{Fe}_{85.2}\text{Si}_2\text{B}_8\text{P}_4\text{Cu}_{0.8}$ hetero-amorphous alloy. Atomic clusters are seen in the encircled area.

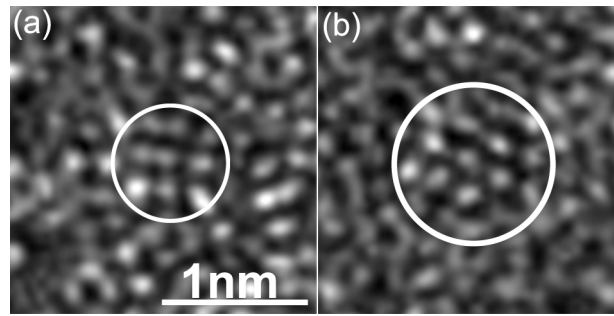


FIG. 3. Examples of (a) [100]-oriented and (b) [111]-oriented bcc-Fe-like clusters. Crossed lattice fringes of ~ 0.2 nm in spacing are seen, while those are distorted.

illuminated along their atomic columns. However, it should be emphasized that even under such condition cluster regions with four-fold or six-fold atomic arrangements are locally observed as indicated by double-arrowheads, implying existence of stable crystalline bcc-Fe clusters¹² with a considerable volume fraction in the alloy. In the structure simulation of Fe-B amorphous alloys with near eutectic compositions by Mykol *et al.*,¹³ regions of bcc-Fe clusters are formed together with icosahedral-Fe and polytetrahedral Fe-B cluster regions, in agreement with a Voronoi polyhedral analysis of the eutectic Fe-B alloy from an electron diffraction study.¹¹ The observed onion-like and deformed-crystal-like regions are considered to be image projections of these local clusters. A rigorous image simulation has to be made for such characteristic types of local crystalline clusters in order to understand all the observed important images of local clusters.

Magnified images of [100]-oriented and [111]-oriented bcc-Fe (or Fe-based alloy) clusters are shown in Figs. 3(a) and 3(b), respectively. As can be seen, local crossed-lattice fringes of ~ 0.2 nm in spacing extend over 1 nm, while those are heavily distorted. Such images imply that inter-atomic distance and cross-angles between atomic planes of these clusters must be close to those of bcc-Fe. It should be noted that, according to the preceding image simulation studies, such locally ordered regions are not reproduced by assuming a dense random packing (DRP) model structure.^{10,11,14} The present HRTEM observation strongly supports the existence of bcc-Fe like clusters in the as-quenched FeSiBPCu alloy.

Figure 4 shows scanning NBED patterns including weak diffraction spots. The pattern shown in Fig. 4(a) is close to $\sim [001]_{\text{bcc-Fe}}$ zone. Reflections indicated by arrowheads having a lattice spacing of ~ 0.2 nm correspond to 110 reflections of bcc-Fe (also can be seen in Fig. 4(b)). These NBED patterns from the cluster regions are usually deformed and asymmetric in their spot-intensities with respect to the central spot due to their local lattice distortion. The distribution of interplanar spacing (spot distance) is at most $\sim 7\%$. Similarly, double-arrowheads in Fig. 4(c) suggest 200 reflections of bcc-Fe with a lattice spacing of ~ 0.14 nm. Thus, the observation of these NBED patterns is also a strong evidence of existence of crystalline bcc-Fe clusters in the as-quenched melt-spun ribbon. Among the dense atomic clusters exist in the as-quenched alloy it is presumed that a part

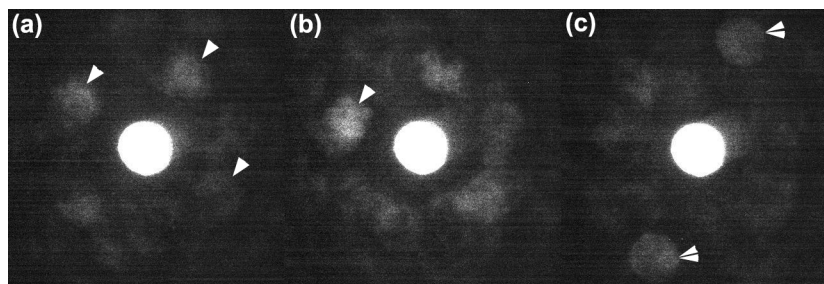


FIG. 4. Scanning NBED patterns including weak diffraction spots. Probe size is ~ 0.1 nm with beam convergence semi-angle of ~ 3 mrad (a $5 \mu\text{m}$ -sized condenser aperture was used). (a) beam incidence $\sim [001]_{\text{bcc-Fe}}$, (b) and (c) include 110 (an arrowhead) and 200 (double-arrowheads) reflections of α -Fe, respectively.

of the clusters with structures close to the bcc-Fe must contribute to high-density α -Fe nanocrystals produced by post-annealing.

In summary, a combination of modern C_s -corrected HRTEM and scanning NBED unambiguously revealed a formation of a hetero-amorphous structure including high-density crystalline clusters in the as-quenched $\text{Fe}_{85.2}\text{Si}_2\text{B}_8\text{P}_4\text{Cu}_{0.8}$ alloy with the high Fe content. The size of the clusters are typically ~ 1 nm in diameter. A part of these clusters is bcc-Fe-like in respect of interplanar spacing and symmetry of NBED patterns as well as atomic image contrast. Our next step is to clarify growing process of these “pre-existing” bcc-Fe clusters on annealing, which would be a key to unveil the formation process of high-density α -Fe nanocrystals with excellent soft magnetic properties.

ACKNOWLEDGMENTS

This work was supported by the “Tohoku Innovative Materials Technology Initiatives for Reconstruction (TIMT)” funded by the Ministry of Education, Culture, Sports, Science and Technology (MEXT) and Reconstruction Agency, Japan. KS wishes to thank Prof. N. Nishiyama and Dr. A. Hirata of Tohoku University for invaluable comments.

- ¹ Y. Yoshizawa, S. Oguma, and K. Yamauchi, *J. Appl. Phys.* **64**, 6044 (1988).
- ² K. Suzuki, A. Makino, N. Kataoka, A. Inoue, and T. Masumoto, *Mater. Trans. JIM* **32**, 93 (1991).
- ³ M. A. Willard, D. E. Laughlin, M. E. McHenry, D. Thoma, K. Sickafus, J. O. Cross, and V. G. Harris, *J. Appl. Phys.* **84**, 6773 (1998).
- ⁴ A. Makino, H. Men, T. Kubota, K. Yubuta, and A. Inoue, *Mater. Trans.* **50**, 204 (2009).
- ⁵ A. Makino, H. Men, T. Kubota, K. Yubuta, and A. Inoue, *J. Appl. Phys.* **105**, 07A308 (2009).
- ⁶ P. Sharma, X. Zhang, Y. Zhang, and A. Makino, *Scripta Mater.* **95**, 3 (2015).
- ⁷ K. Sato, M. Mizuguchi, R. Tang, J.-G. Kang, M. Ishimaru, K. Takanashi, and T. J. Konno, *Appl. Phys. Lett.* **101**, 191902 (2012).
- ⁸ M.-H. Kwon, B.-S. Lee, S. N. Bogle, L. N. Nittala, S. G. Bishop, J. R. Abelson, S. Raoux, and K.-B. Kim, *Appl. Phys. Lett.* **90**, 021923 (2007).
- ⁹ M. M. J. Treacy, J. M. Gibson, L. Fan, D. J. Paterson, and I. McNulty, *Rep. Prog. Phys.* **68**, 2899 (2005).
- ¹⁰ Y. Hirotsu, T. Ohkubo, and M. Matsushita, *Microsc. Res. Tech.* **40**, 284 (1998).
- ¹¹ A. Hirata, Y. Hirotsu, T. Ohkubo, T. Hanada, and V. Z. Bengus, *Phys. Rev. B* **74**, 214206 (2006).
- ¹² Y. Hirotsu and R. Akada, *Jpn. J. Appl. Phys.* **23**, L479 (1984).
- ¹³ M. Aykol, A. O. Mekhrabov, and M. V. Akdeniz, *Acta Mater.* **57**, 171 (2009).
- ¹⁴ T. Hamada and F. E. Fujita, *Jpn. J. Appl. Phys.* **25**, 318 (1986).